



**BIO 402**

**END SEMESTER REPORT**

---

# **Simulate computational models of astrocyte-neuron interaction**

---

**AUTHOR**

Antony Kiran K David  
20181083

BS-MS student, IISER Pune

**SUPERVISOR**

Dr Suhita Nadkarni

Division of Biology, IISER Pune

August 2021 – November 2021

## Table of Contents

List of Figures.....	3
List of Tables.....	3
Abstract.....	4
Module 1.....	4
Introduction.....	4
The Hodgkin-Huxley model.....	4
Methods.....	6
Simulating the Hodgkin-Huxley model:.....	6
Plotting the bifurcation diagram:.....	6
Results and Discussion.....	6
Hodgkin-Huxley model could reproduce various observations attributed to typical neuronal spiking.....	6
Conclusions and Future Prospects.....	9
Module 2.....	10
Introduction.....	10
The Li-Rinzel Model.....	10
Langevin approximation of Li-Rinzel model:.....	11
Methods.....	11
Simulating the deterministic Li-Rinzel model:.....	11
Langevin approximation of the Li-Rinzel model:.....	12
Results and discussion.....	12
The Deterministic Li-Rinzel model captures the calcium spike in response to $IP_3$ stimulation....	12
The Langevin approximation of the Li-Rinzel model was able to capture the stochasticity of the $IP_3R$ channel opening.....	12
Conclusions and Future prospects.....	13
Acknowledgements.....	13
References.....	13

## List of Figures

Figure 1: Approximation of an axonal patch in the Hodgkin-Huxley model .....	4
Figure 2: Circuit diagram representation of the Hodgkin-Huxley model .....	5
Figure 3: Simulating the Hodgkin-Huxley model. (A) Dynamics of the three gating variables. (B) Application of input current. (C) Membrane potential varying with time. The red arrow denotes the time of application of stimulating current. ....	7
Figure 4: (A) Stimulating with $3 \mu\text{A}/\text{cm}^2$ current for 5 s, 10 s apart. (B) Stimulating with $3 \mu\text{A}/\text{cm}^2$ and $15 \mu\text{A}/\text{cm}^2$ current for 5 s, 10 s apart. ....	8
Figure 5: Maximum membrane voltage in the initial spike with varying input current .....	8
Figure 6: Bifurcation diagram .....	9
Figure 7: : Calcium dynamics captured by the deterministic Li-Rinzel model. Here the stimulus was provided between the 60 <sup>th</sup> and the 90 <sup>th</sup> s. ....	12
Figure 7: : Calcium dynamics captured by the deterministic Li-Rinzel model. Here the stimulus was provided between the 60 <sup>th</sup> and the 90 <sup>th</sup> s. ....	12
Figure 8: Calcium peak histogram for the Langevin approximation of the Li-Rinzel model .....	12
Figure 8: Calcium peak histogram for the Langevin approximation of the Li-Rinzel model .....	12

## List of Tables

Table 1: Parameters of the Hodgkin-Huxley Model. Here the membrane capacitance, $C = 1 \mu\text{F}/\text{cm}^2$ and membrane voltage set to 0 mV. ....	6
Table 2: Parameters used in the Li-Rinzel model with the initial value of $Ca_2^+$ and $h$ to be zero. ....	11

## Abstract

Recent studies have shed light on the bidirectional communication between astrocytes and neurons for the brain's normal functioning. This bidirectional communication is thought to be occurring through the Calcium-dependent release of gliotransmitters. Anup and Nadkarni (1) have described a detailed biophysical model that can quantitatively describe this gliotransmitter release by a single astrocyte process in response to a wide range of synaptic activity. This project aims to reproduce the results of the work done by Anup and Nadkarni by implementing the model using python. Since this is a learning project, the report was divided into two modules (for ease of reporting). The first module simulates the classic Hodgkin-Huxley model of neuronal spiking, followed by the Li-Rinzel model for calcium dynamics in neurons and its stochastic modelling in the 2<sup>nd</sup> module.

## Module 1

### Introduction

The Classic experiment of Hodgkin and Huxley in 1952(2) on the giant squid axon led to the discovery of 3 main ion currents, viz,  $\text{Na}^+$ ,  $\text{K}^+$  and a leak current mainly consisting of  $\text{Cl}^-$  ions. These ionic currents were controlled by specific voltage-dependent, one for sodium and one for potassium. The other channels that are not specified explicitly are responsible for the leak current. This module simulates the classic space clamped Hodgkin-Huxley model for a patch of axonal membrane.

### The Hodgkin-Huxley model(3)

The Hodgkin-Huxley model is a simple approximation of an axonal patch with only three types of channels. Here the semipermeable cell membrane separates the cell's interior from the extracellular material, acting as a capacitor, as shown in Figure 1.

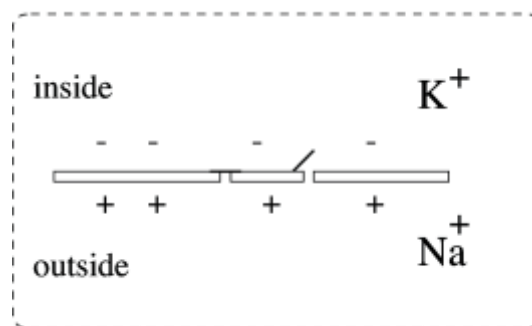


Figure 1: Approximation of an axonal patch in the Hodgkin-Huxley model

Now since the cell membrane acts as a capacitor, if an input current is  $I(t)$  is passed into the cell, it may either add charge to the capacitor or leak through the channels in the cell membrane. The axonal membrane has  $\text{Na}^+/\text{K}^+$  ATPase, which maintains the ion concentration inside the cell different from the extracellular space. The potential difference generated by the difference in ion concentration is similar to the role of the battery in an electric circuit.

Hence the axonal patch may be approximated to an electric circuit with a capacitance  $C$ , resistance  $R$ , which can be thought of as the resistance of leak channel and two variable resistance, one representing Sodium and Potassium channels, respectively. This is represented in the circuit diagram shown in Figure 2. In the diagram, the earthing represents that the resting membrane potential is set to be zero.

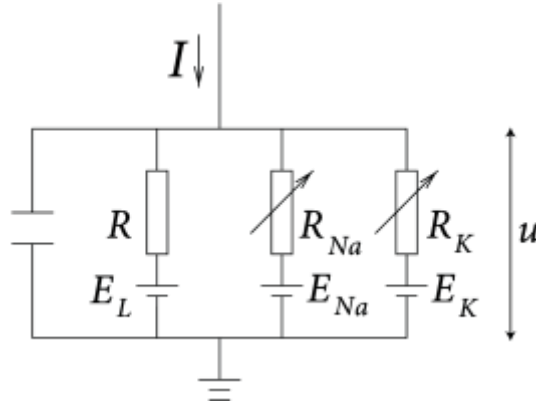


Figure 2: Circuit diagram representation of the Hodgkin-Huxley model

Putting all these into mathematical terms, we can say that when a current stimulates the patch  $I(t)$ , it will be split into two currents: a capacitive current  $I_c$ , which charges the capacitor  $C$  and other components  $I_k$  which pass through the ion channels.

Thus we can say,

$$I(t) = I_c(t) + \sum_k I_k(t) \quad (1)$$

Since the Hodgkin-Huxley model describes only three types of channels viz.,  $\text{Na}^+$ ,  $\text{K}^+$  and an unspecific leak channel with resistance  $R$ , the summation over  $k$  run over all these ion channels.

As capacitance is defined as  $C = \frac{Q}{u}$ , where  $Q$  is the charge, and  $u$  is the voltage across the capacitor,

the stimulating current  $I_c$  can be written as  $I_c = c \frac{du}{dt}$ .

Hence equation (1) can be written as:

$$c \frac{du}{dt} = - \sum_k I_k(t) + I(t) \quad (2)$$

In terms of the axonal patch,  $u$  represents the voltage across the cell membrane and  $\sum_k I_k(t)$  is the sum of the ionic currents that is passing through the membrane.

In the Hodgkin-Huxley framework, the three channels are characterised by their resistance or

conductance. The leakage channel is described by a voltage-independent conductance  $g_L = \frac{1}{R}$

whereas the conductance of the other two channels is voltage-dependent. The opening of the sodium and potassium channels is probability dependent, and when all the channels are open, they conduct currents with a maximum capacity of  $g_{Na}$  or  $g_K$ , respectively. In the normal physiological state, some channels are closed. The probability that a channel is open is described by additional parameters called gating variables viz.,  $m$ ,  $n$  and  $k$ .

The sodium channels are controlled by the combined action of the  $m$  and  $h$  gating variables. The variable  $n$  controls the opening and closing of the potassium channels. By considering this, Hodgkin and Huxley characterised the current components as:

$$\sum_k I_k = g_{Na} m^3 h (u - E_{Na}) + g_K n^4 (u - E_K) + g_L (u - E_L) \quad (3)$$

Here  $E_{Na}, E_K, E_L$  are called the reversal potentials. Both the reversal potential as well as the conductance are determined empirically. The values of the parameters described by Hodgkin and Huxley where the resting membrane potential is zero is summarised in Table 1.

				$n$	$0.1 - 0.01u$	$0.125e^{-u/80}$	
				$m$	$\frac{e^{1-0.1u} - 1}{2.5 - 0.1u}$	$4e^{-u/18}$	(mV)
$g_x$	$Na$	115	120				
	$K$	-12	36				
	$L$	10.6	0.3				
(mS/cm <sup>2</sup> )		$\alpha_x$ (mV)	$\beta_x$ (mS/cm <sup>2</sup> )	$h$	$0.07e^{-u/20}$	$\frac{1}{e^{3-0.1u} + 1}$	

Table 1: Parameters of the Hodgkin-Huxley Model. Here the membrane capacitance,  $C = 1 \mu\text{F}/\text{cm}^2$  and membrane voltage set to 0 mV.

The three gating variables evolve according to the differential equation described below:

$$\begin{aligned}
 \dot{m} &= \alpha_m(u)(1 - m) - \beta_m(u)m \\
 \dot{n} &= \alpha_n(u)(1 - n) - \beta_n(u)n \\
 \dot{h} &= \alpha_h(u)(1 - h) - \beta_h(u)h
 \end{aligned} \tag{4}$$

Here  $\dot{m}$  denotes  $\frac{dm}{dt}$  and so on for n and h. The functions  $\alpha$  and  $\beta$  are described in Table 1 and are empirical functions that fit the data collected from the giant axon of the squid by Hodgkin and Huxley.

## Methods

### Simulating the Hodgkin-Huxley model:

The explicit Euler method was used to simulate the equations described above using custom python scripts. The simulations were done for 100 ms with a time step of 0.01 ms for integration. The stimulus (input current) of  $10 \mu\text{A}/\text{cm}^2$  was provided from 10<sup>th</sup> ms to the end of the simulation.

### Plotting the bifurcation diagram:

The model was stimulated with input currents varying from 1 to 300  $\mu\text{A}/\text{cm}^2$  in steps of 1  $\mu\text{A}/\text{cm}^2$  throughout the simulation, and the maximum and minimum membrane voltages were plotted for the last 20 ms in each run to obtain the bifurcation diagram.

## Results and Discussion

### Hodgkin-Huxley model could reproduce various observations attributed to typical neuronal spiking.

A characteristic spike train was observed after the simulation. The spiking in the membrane potential was correlated with the time of application of the stimulating current. The plots for the gating variables' dynamics and membrane potential are shown in Figure 3.

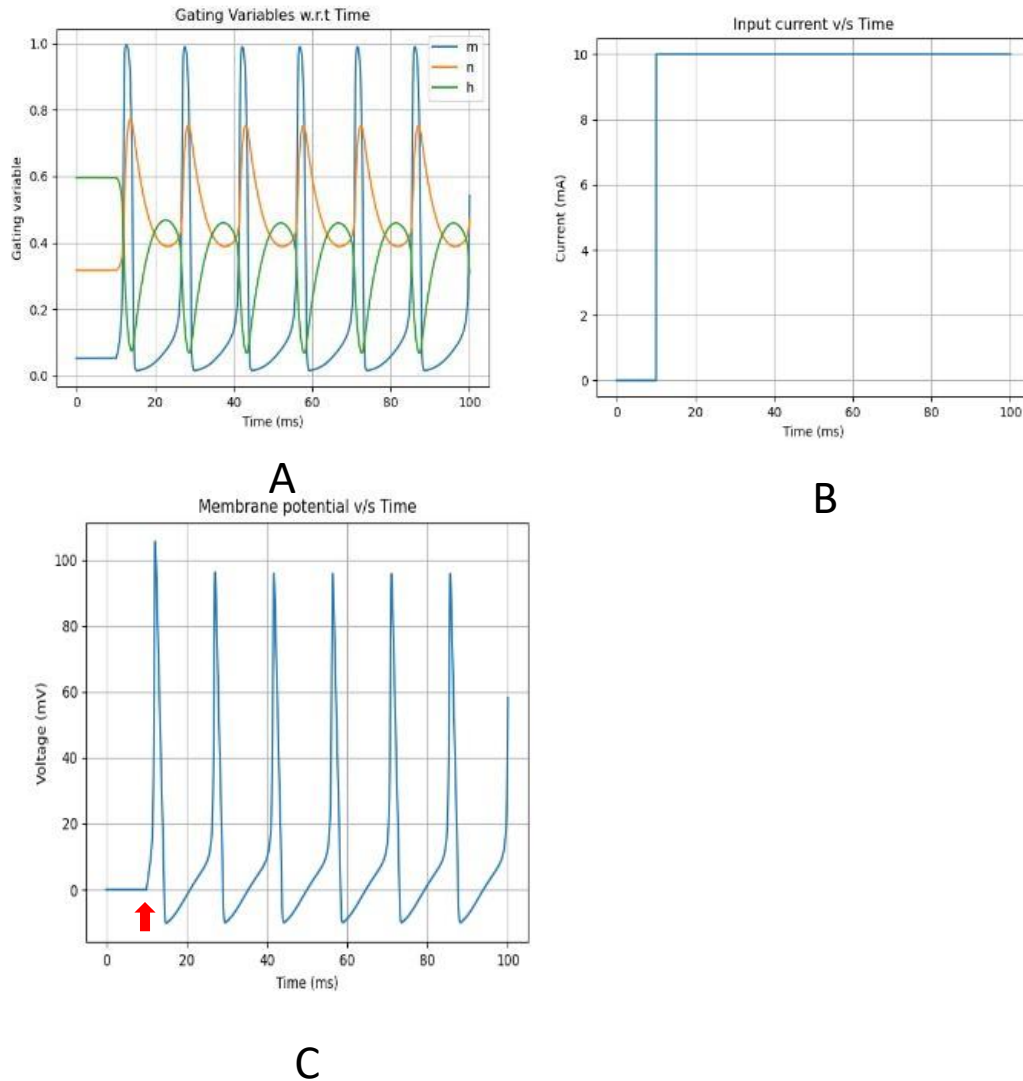


Figure 3: Simulating the Hodgkin-Huxley model. (A) Dynamics of the three gating variables. (B) Application of input current. (C) Membrane potential varying with time. The red arrow denotes the time of application of stimulating current.

In the case of constant current input, we could observe regular spiking of the membrane potential with maximum value at the first spike. The interval seen between two spikes is called the refractory period. This is because the sodium channels will be inactivated at this time, and hence the cell cannot respond to the input current.

The maximum value of membrane potential is seen in the first spike. This can be attributed to the phenomenon called refractoriness. In this model of neuronal firing, the maximum value of the membrane potential depends on the amplitude of the stimulating current. Since we have a constant input current, the 2nd spike initiated during the refractory period, a higher amplitude current is required to get the same level of membrane potential. This can be seen more clearly in Figure 4. Here a much stronger current is needed for getting a second spike during the hyperpolarisation phase.

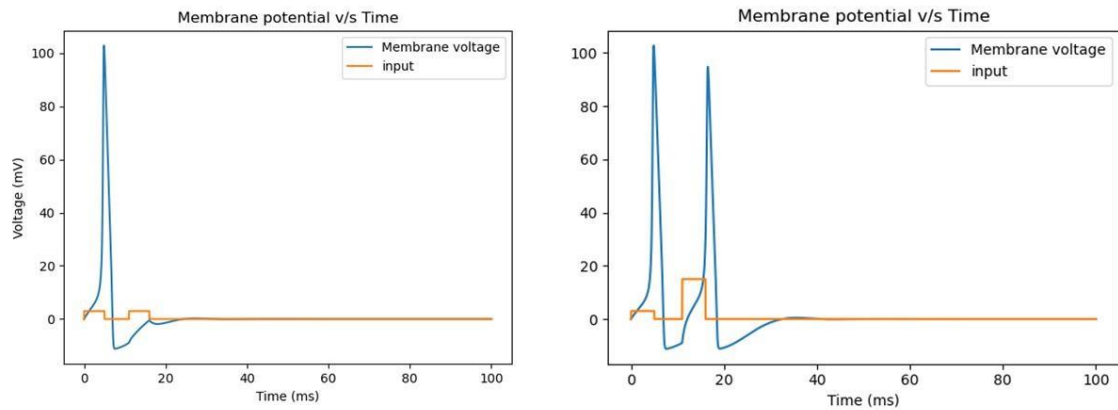


Figure 4: (A) Stimulating with  $3 \mu\text{A}/\text{cm}^2$  current for 5 s, 10 s apart. (B) Stimulating with  $3 \mu\text{A}/\text{cm}^2$  and  $15 \mu\text{A}/\text{cm}^2$  current for 5 s, 10 s apart.

It was also observed that there is a particular current threshold below which we could not obtain the spiking activity. For the parameters described in this model, this threshold was found to be between  $2\text{-}3 \mu\text{A}/\text{cm}^2$ . The maximum voltage in response to varying input current is shown in Figure 5.

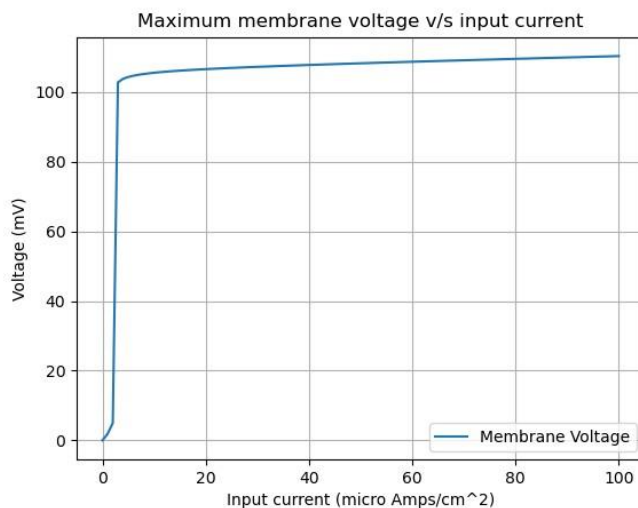


Figure 5: Maximum membrane voltage in the initial spike with varying input current

The bifurcation diagram for constant continuous current is shown here. We can see that at very low currents, the voltage has a stable fixed point. As the value of current increases, voltage executes a longer trajectory to reach its stable fixed point. After a critical current value  $\sim 2.3 \mu\text{A}/\text{cm}^2$ , the stable node disappears, and a stable spiral appears in the phase diagram. Now there is an unstable node inside the stable loop. This behaviour resembles a supercritical Hopf bifurcation, i.e., a stable node changes to an unstable node surrounded by a stable spiral. The voltage value oscillates between a minimum and maximum value

After this, when we increase the current further, the radius of the stable spiral decreases and finally collapses to a stable fixed point at another critical current value  $\sim 160 \mu\text{A}/\text{cm}^2$ . This is a subcritical Hopf bifurcation, as a stable spiral disappears, and a stable fixed node appears when the parameter value increases. The fixed point is a stable spiral, as noted from the simulations. The minimum and maximum

values of the voltage are the same, implying that the voltage remains fixed even though a stimulating current is provided. Also, note that the stable voltage is a non-zero value ( $\sim 25$  mV and increasing).

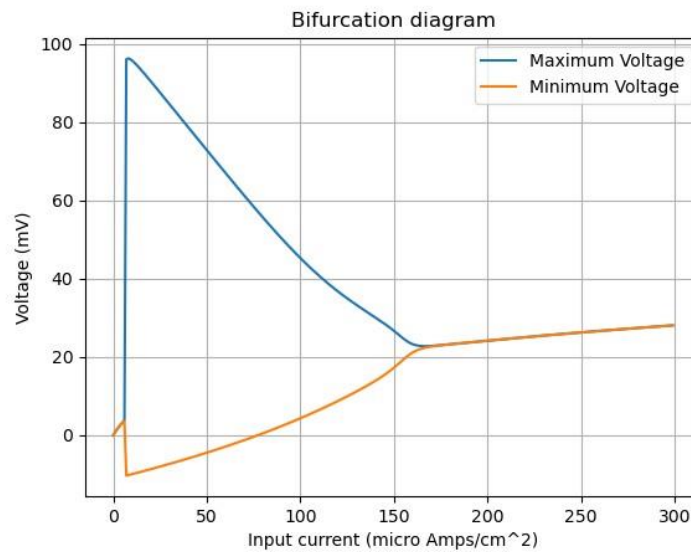


Figure 6: Bifurcation diagram

## Conclusions and Future Prospects

Even though the Hodgkin-Huxley is a simple approximation of the spiking behaviour of an axonal patch, it could reproduce some of the classical characters attributed with a typical neuronal spiking. This report summarises a few of them, and there are a lot of special cases that can be tried and tested using this model, which is beyond the scope of this study. Thus this has become one of the successful theoretical models describing neuronal spiking. All the parameters were estimated from various experiments by the original authors cited in the appropriate sections and have not been validated in the present study.

## Module 2

### Introduction

In 1992, De Young and Keizer proposed the first theoretical model for the agonist-induced  $Ca^{2+}$  oscillations based on the kinetics of 1,4,5-trisphosphate ( $IP_3$ ) and the gating of the  $IP_3$  Receptor ( $IP_3R$ ). This model assumes that the  $IP_3R$  has three independent subunits for conducting. Each subunit has three binding sites, 2 for Calcium and one for  $IP_3$ . The binding of Calcium to one of the sites activates and to the other deactivates the channel. Thus there are  $2^3$  states for each subunit. All the subunits must have Calcium bound to the activation site and  $IP_3$  to the  $IP_3$  site for the channel to conduct. Though this model could reliably capture the complex gating dynamics, the number of variables was relatively high. Li and Rinzel proposed a relatively simple approximation of this model in 1994. From the observation that the De Young-Keizer model was symmetric in some bound states, the  $IP_3$  binding is at least 200 times faster than  $Ca^{2+}$  activation binding while this in-turn is at least 10 times faster than  $Ca^{2+}$  deactivation binding. Thus the De Young-Keizer model was approximated to a system of 2 coupled ordinary differential equations.

This module will consist of simulating the deterministic Li-Rinzel model for a patch of a cell membrane. Recent high-resolution microscopic recordings suggest that these channels are spatially organised as clusters. The collective opening and closing of these channels are responsible for the  $Ca^{2+}$  puffs observed in experiments. Since mathematical models are directly based on these experiments, deterministic Li-Rinzel may be insufficient to model the stochastic nature of these experimental observations due to the relatively small number of calcium release channels in a patch. Hence the Langevin approximation of the Li-Rinzel model proposed by Shuai et al. to introduce stochasticity in the deterministic model will be simulated in the later sections of this module.

### The Li-Rinzel Model(4)

The Li-Rinzel model for agonist-induced calcium dynamics in the cytosol consists of 2 coupled ordinary differential equations described below:

$$\frac{d[Ca^{2+}]}{dt} = -J_{channel} - J_{pump} - J_{leak} \quad (5)$$

$$\frac{dh}{dt} = \alpha h(1 - h) - \beta_h h \quad (6)$$

Here  $J_{channel}$  represents the flux of calcium ions from the ER to the intracellular space through the  $IP_3R$  channels,  $J_{pump}$  represents the flux of Calcium being pumped out from the intracellular space to the ER and  $J_{leak}$  represents the flux of Calcium being leaked into the intracellular space from the ER. They are given by the expressions below:

$$J_{channel} = c_1 v_1 m_{\infty}^3 n_{\infty}^3 h^3 ([Ca^{2+}] - [Ca^{2+}]_{ER}) \quad (7)$$

$$J_{pump} = k \frac{V_3 [Ca^{2+}]^2}{3 + [Ca^{2+}]^2} \quad (8)$$

$$J_{leak} = c_1 v_1 ([Ca^{2+}] - [Ca^{2+}]_{ER}) \quad (9)$$

Where,

$$m_{\infty} = \frac{[IP_3]}{[IP_3] + d_1}$$

$$n^\infty = \frac{[Ca^{2+}]}{[Ca^{2+}] + d_5}$$

$$\alpha^h = a_2 d_2 \frac{[IP_3] + d_1}{[IP_3] + d_3}$$

$$\beta_h = a_2 [Ca^{2+}]$$

The parameters used in the model are summarised in Table 2.

### Parameter Value

c1	0.185
v1	6 s <sup>-1</sup>
v2	0.11 s <sup>-1</sup>
v3	0.9 μM s <sup>-1</sup>
k3	0.1 μM
d1	0.13 μM
d2	1.049 μM
d3	0.9434 μM
d5	0.08234 μM
a2	0.2 μM <sup>-1</sup> s <sup>1</sup>
$\frac{[Ca^{2+}]_{ER}}{c1}$	$\frac{c0 - [Ca^{2+}]}{c1}$
c0	2.0 μM

Table 2: Parameters used in the Li-Rinzel model with the initial value of  $[Ca^{2+}]$  and  $h$  to be zero.

### Langevin approximation of Li-Rinzel model:(4)

In the Langevin approximation of the Li-Rinzel model, the stochastic behaviour of the channel is captured by adding a gaussian white noise term to the equation for a fraction of open channels as expressed in equation (10). Equation (11) describes the formula for generating the zero mean, uncorrelated Gaussian white noise. Hence the Langevin approach indicates that the stochastic dynamics of the IP<sub>3</sub>R channels can be treated as deterministic dynamics distributed by Gaussian white noise.

$$\frac{d}{dt} h_i = \alpha^h (1 - h_i) - \beta_h h_i + G_{hi}(t) \quad (10)$$

$$\langle G_{hi}(t) G_{hj}(t') \rangle = \alpha_h (1 - h_i) - \beta_h h_i \delta(t - t') \delta_{ij} \quad (11)$$

Where  $i, j = 1, 2, 3$

For simplifying the problem, we can write  $h_1 h_2 h_3$  as  $h^3$ , assuming that the three gates of the IP<sub>3</sub>R are identical. This creates a gain in computational speed by a factor of 3.

## Methods

### Simulating the deterministic Li-Rinzel model:

The `odeint()` function of the SciPy(6) package in Python 3.6.6(7) was used to numerically solve the equations described in equations (5) and (6) with a time step of integration as 0.001 s. The entire

simulation was run for 100 s using  $[IP_3]$  as the stimulating parameter. The stimulus was given between the 60<sup>th</sup> and 90<sup>th</sup> s with an  $IP_3$  concentration of 0.5  $\mu$ M.

#### Langevin approximation of the Li-Rinzel model:

The equations described in equations (5) and (10) were solved using the `odeint()` function of the SciPy package in Python 3.6.6, as discussed in the previous section with a timestep of integration 0.001 s. The gaussian white noise term was generated using the `normal()` function in the NumPy(8) package in python using default parameters. It was run for 400 independent trials to capture the stochastic behaviour, and a histogram was plotted with the peak amplitude of calcium spike in each run. All simulations were run for at least 50 s before applying the stimulus (0.5  $\mu$ M of  $IP_3$ ). A scaling factor was introduced to match the random term generated to the values of the h gating variable. A check was performed after every simulation to check if the value of h goes beyond 0 and 1.

### Results and discussion

The Deterministic Li-Rinzel model captures the calcium spike in response to  $IP_3$  stimulation.

A characteristic spike of calcium concentration was observed upon  $IP_3$  application. Though the model started with an initial calcium concentration of 0  $\mu$ M, it soon reached an equilibrium value within seconds after the start of the simulation. The concentration returned to this equilibrium value soon after the stimulating  $IP_3$  was removed. This is the resting calcium concentration in the cytosol. The calcium dynamics captured from the model is shown in Figure 7.

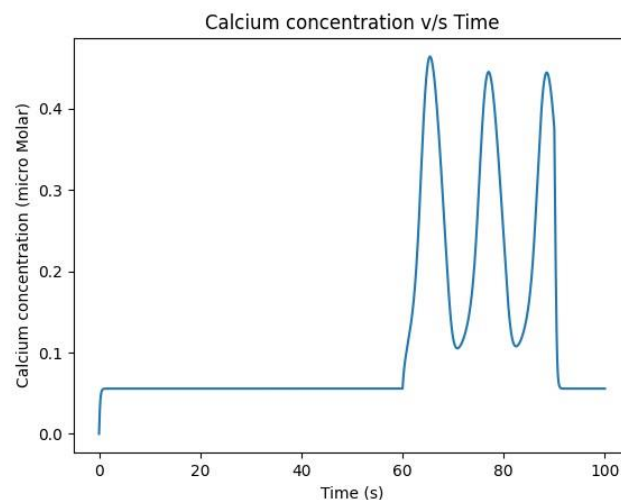


Figure 7: : Calcium dynamics captured by the deterministic Li-Rinzel model. Here the stimulus was provided between the 60<sup>th</sup> and the 90<sup>th</sup> s.

Figure 8: : Calcium dynamics captured by the deterministic Li-Rinzel model. Here the stimulus was provided between the 60<sup>th</sup> and the 90<sup>th</sup> s.

The Langevin approximation of the Li-Rinzel model was able to capture the stochasticity of the  $IP_3$ R channel opening.

The histogram plotted for the maximum peaks of calcium concentration of 400 independent trials had a normal distribution, as shown in Figure 8.

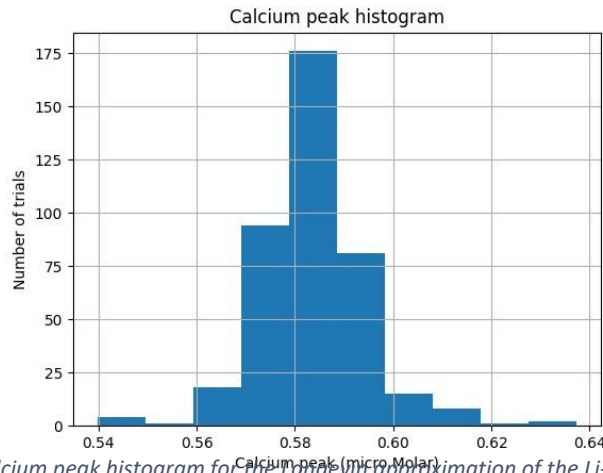


Figure 9: Calcium peak histogram for the Langevin approximation of the Li-Rinzel model

Figure 10: Calcium peak histogram for the Langevin approximation of the Li-Rinzel model

## Conclusions and Future prospects

The Langevin approximation of the Li-Rinzel model is a computationally less demanding model for capturing the stochastic behaviour of the IP<sub>3</sub>R channels. It can be used to model various complex calcium dynamics in different cell types. Pillai et al. 2019(1) has used the Langevin approximation to create a detailed biophysical model of gliotransmitter release in response to calcium signalling in a tripartite synapse. The next step of this project would be implementing the model proposed by Pillai et al. and reproducing their results. This can further be expanded by modelling how this gliotransmitter release affects synaptic signalling.

## Acknowledgements

This project was done as part of the BIO 401 Semester project as part of the BS-MS program at IISER Pune. The project was brought to completion based on the discussion with my supervisor Dr Suhita Nadkarni. I would like to thank Dr Nadkarni for her constant support in the lab.

I would like to thank my lab members and friends for their constant support and help during the project term. I would like to thank Abel Shibu and Bharat Krishnan for the help they have given me in different aspects of the project.

All codes used in the project will be made available in the repository <https://github.com/antonykiran10/CompNeuroLab>. All the simulations were run on a workstation with Intel® Xeon(R) CPU E5-1620 v3 processor and 32 GB of RAM running Ubuntu 18.04.6 LTS.

## References

1. Pillai AG, Nadkarni S. Amyloid pathology disrupts gliotransmitter release in astrocytes [Internet]. Neuroscience; 2019 Jun [cited 2021 Aug 5]. Available from: <http://biorxiv.org/lookup/doi/10.1101/679860>
2. Hodgkin AL, Huxley AF. A quantitative description of membrane current and its application to conduction and excitation in nerve. The Journal of Physiology. 1952 Aug 28;117(4):500–44.

3. Gerstner W, Kistler WM. Spiking neuron models: single neurons, populations, plasticity. Cambridge, U.K. ; New York: Cambridge University Press; 2002. 480 p.
4. Shuai J-W, Jung P. Stochastic Properties of Ca<sup>2+</sup> Release of Inositol 1,4,5-Trisphosphate Receptor Clusters. *Biophysical Journal*. 2002 Jul 1;83(1):87–97.
5. Li Y-X, Rinzel J. Equations for InsP<sub>3</sub> Receptor-mediated [Ca<sup>2+</sup>]<sub>i</sub> Oscillations Derived from a Detailed Kinetic Model: A Hodgkin-Huxley Like Formalism. *Journal of Theoretical Biology*. 1994 Feb;166(4):461–73.
6. SciPy [Internet]. [cited 2021 Dec 1]. Available from: <https://scipy.org/>
7. Welcome to Python.org [Internet]. Python.org. [cited 2021 Dec 1]. Available from: <https://www.python.org/>
8. NumPy [Internet]. [cited 2021 Dec 1]. Available from: <https://numpy.org/>